The *ovo* gene required for cuticle formation and oogenesis in flies is involved in hair formation and spermatogenesis in mice

Xing Dai, Christopher Schonbaum, Linda Degenstein, et al.

Genes Dev. 1998 12: 3452-3463
Access the most recent version at doi:10.1101/gad.12.21.3452

The *ovo* gene required for cuticle formation and oogenesis in flies is involved in hair formation and spermatogenesis in mice

Xing Dai,[2] Christopher Schonbaum,[2] Linda Degenstein,[1,2] Wenyu Bai,[2] Anthony Mahowald,[2,3] and Elaine Fuchs[1,2,3]

[1]Howard Hughes Medical Institute, [2]Department of Molecular Genetics and Cell Biology, [3]Committee on Developmental Biology, The University of Chicago, Chicago, Illinois 60637 USA

The *Drosophila svb/ovo* gene gives rise to differentially expressed transcripts encoding a zinc finger protein. *svb/ovo* has two distinct genetic functions: *shavenbaby* (*svb*) is required for proper formation of extracellular projections that are produced by certain epidermal cells in late-stage differentiation; *ovo* is required for survival and differentiation of female germ cells. We cloned a mouse gene, *movo1* encoding a nuclear transcription factor that is highly similar to its fly counterpart in its zinc-finger sequences. In mice, the gene is expressed in skin, where it localizes to the differentiating cells of epidermis and hair follicles, and in testes, where it is present in spermatocytes and spermatids. Using gene targeting, we show that *movo1* is required for proper development of both hair and sperm. *movo1*$^{-/-}$ mice are small, produce aberrant hairs, and display hypogenitalism, with a reduced ability to reproduce. These mice also develop abnormalities in kidney, where *movo1* is also expressed. Our findings reveal remarkable parallels between mice and flies in epidermal appendage formation and in germ-cell maturation. Furthermore, they uncover a phenotype similar to that of Bardet–Biedl syndrome, a human disorder that maps to the same locus as human *ovo1*.

[*Key Words*: *ovo*; skin; hair; spermatogenesis; knockout mice]

Received August 3, 1998; revised version accepted September 9, 1998.

Conservation of molecular mechanisms throughout evolution, in particular, between flies and mammals, is not unprecedented. In recent years, numerous cases have been reported in which mammalian homologs of developmentally important *Drosophila* genes perform similar functions and participate in similar pathways as their fly relatives. As the organ separating the animal body from its environment, skin/skin appendages in both flies and mice carry out essential protective and sensory functions. Comparative studies suggest that genes involved in patterning the *Drosophila* larval epidermis, including those in the *decapentaplegic*, *wingless*, and *Sonic hedgehog* pathways, are also utilized in patterning the mammalian skin (for review, see Fuchs 1995; Willert and Nusse 1998). However, little is known about the molecular and functional conservation of the many *Drosophila* genes implicated in epidermal development, cuticle formation, and cuticle-denticle differentiation (for review, see Martinez Arias 1993). Less conservation among these processes has been anticipated, given the fact that in fly, a single-layered epidermis produces and secretes cuticle and forms denticles. In contrast, the surface ectoderm of mammals is the progenitor of epidermis and hair follicles, each composed of multiple, differentiating cell layers.

Germ-line sex determination is another process strikingly different between flies and mice. In *Drosophila*, male is the default state of germ-line development (Granadino et al. 1993), and the female pathway requires both an inductive signal from soma and an autonomous signal dependent upon the X chromosome to autosome ratio (for review, see Wei and Mahowald 1994; Cline and Meyer 1996; Lin 1997). In mammals, germ-line sex determination depends on nonautonomous and autonomous factors, but in a very different way from *Drosophila* (for review, see Bogan and Page 1994; McLaren 1995; Capel 1998).

The *ovo* locus in *Drosophila* is interesting in that it encodes proteins involved in both of these evolutionarily diverse processes. The *ovo* locus produces multiple transcripts that originate from at least two promoters and share largely overlapping coding sequences (Garfinkel et al. 1994; Mevel-Ninio et al. 1995). Defects affecting either upstream regulatory elements or the coding portion of the *ovo* locus result in the *shavenbaby* (*svb*) pheno-

[3]Corresponding author.
E-MAIL lain@midway.uchicago.edu; FAX (773) 702-0141.

type (Wieschaus et al. 1984). Although isolated originally in a search for mutants in larval cuticle patterning, *svb* mutations affect the number and size of denticle setal belts but not the pattern of denticles within a segment. Consistent with this phenotype, *svb* transcripts are detected in those epidermal cells that produce and secrete cuticle that gives rise to these extracellular appendages late in larval development (Garfinkel et al. 1994; Mevel-Ninio et al. 1995). *svb* mutants rarely survive, but the few adult males that do survive display mildly curved bristles (Busson et al. 1983; Oliver et al. 1987), suggesting a role for *svb* in late-stage differentiation of epidermal appendages in larvae and in adult flies.

Recessive-null alleles of the *ovo* locus or mutations affecting downstream regulatory elements result in female-specific sterility caused by loss of embryonic germ cells (Oliver et al. 1987). Less severe mutations produce viable germ-line cells that exhibit defective oogenesis (Oliver et al. 1987) or ovarian tumors with male germline characteristics (Oliver et al. 1990). Dominant *ovo* mutants antagonize wild-type Ovo function and result in abnormal oogenesis (Busson et al. 1983; Mevel-Ninio et al. 1996; Andrews et al. 1998). Consistent with its complex phenotype in the female germ line, *ovo* expression was reported in the germarium, in nurse cells early during oogenesis, and in the germ-line precursor pole cells (Mevel-Ninio et al. 1991; Garfinkel et al. 1994). *ovo* is also expressed in embryonic male germ cells and in germ-line stem cells of adult testis, but no defects in male germ cell production and/or spermatogenesis have been observed (Mevel-Ninio et al. 1995). Thus, *ovo* has been implicated in oogenesis and in female germ-line sex determination, where it is considered a candidate for the target gene of somatic feminization signal (Oliver et al. 1994).

How Ovo and Svb function to regulate such diverse processes remains unexplored. However, several lines of evidence suggest that the protein(s) might act as transcription factors. The carboxy-terminal segment of Ovo/Svb contains four zinc fingers of the C_2H_2 class, a group of proteins known to bind DNA with strong affinity (Mevel-Ninio et al. 1991, 1995; Garfinkel et al. 1992, 1994). In addition, bacterially expressed Ovo/Svb protein has been shown to bind to multiple sites at or near the *ovo* and *ovarian tumor* promoters (Lu et al. 1998). These results are consistent with genetic data that the *ovo* gene is controlled by an autoregulatory mechanism (Garfinkel et al. 1994; Mevel-Ninio et al. 1996), and that *ovo* and *ovarian tumor* function in a common pathway (Pauli et al. 1993). Unequivocal evidence that Ovo/Svb function as transcription factors and the identification of additional candidate genes that might be transcriptionally controlled by Ovo/Svb await further investigation.

Because *ovo/svb* is an example of a single locus with the capacity to carry out two independent functions that are both seemingly diverse across evolution, it is an attractive starting point to rigorously test for similarities between fly and mouse epidermal and/or reproductive differentiation. Here we report the characterization of a mouse *ovo/svb*-related gene and its expression and function. We show that the mouse protein, mOvo1, is not only expressed in similar tissues as its *Drosophila* homolog, but it also plays essential roles in the development of these tissues, in an analogous manner to the fly. We also provide evidence for a possible mechanism of its function, that is, as a transcriptional regulator.

Results

Cloning of a mouse ovo1 *cDNA and the detection of* movo1 *mRNAs in mouse skin but not in ovary*

Using a degenerative PCR strategy, followed by screening of a mouse skin cDNA library, we identified a mouse *ovo* cDNA. The complete sequence and characterization of this cDNA will be reported elsewhere (C. Schonbaum and A. Mahowald, in prep.). Encompassing roughly half of the encoded 30-kD protein, the zinc-finger domains of mouse Ovo share 73% identity with equivalent segments of *Drosophila* Ovo/Svb (Garfinkel et al. 1994) and 94% identity with human Ovo1 (hOvo1; Chidambaram et al. 1997). On the basis of this similarity, we will refer to our sequence as mouse Ovo1a (mOvo1a). As this work was in progress, the sequence of another mouse *ovo* cDNA encoding a similar 31-kD protein was reported (Masu et al. 1998). The reported sequence shares 77% identity with mOvo1 within the zinc-finger domains, and 49% overall; its zinc-finger domains share 98% identity with a second human Ovo protein, hOvo2, reported as an expressed sequence tag (EST) in the database (Hillier et al. 1995). We therefore refer to this sequence as mOvo2. The zinc-finger region of mOvo1a is more similar to *Drosophila* Ovo than mOvo2; however, both mouse Ovo proteins diverge from *Drosophila* Ovo outside these domains. Curiously, *Drosophila* Ovo has a large amino-terminal segment not present in these mammalian Ovo proteins.

To further explore possible parallels between *Drosophila* and mouse *ovo*, we conducted Northern blot analysis on poly(A)$^+$ RNAs isolated from mouse skin and ovary tissues. Under stringent conditions, three transcripts of 3.5, 2.5, and 2.0 kb were detected in adult mouse skin (Fig. 1A). The strongest hybridizing band was 2.0 kb, consistent with the size of our cDNA. The presence of multiple *movo1* transcripts was interesting in light of prior studies on the *Drosophila ovo/svb* gene, where at least three different transcripts have been partially or fully characterized (Mevel-Ninio et al. 1995; Andrews et al. 1998). A complete analysis of the larger transcripts is beyond the scope of the present study.

We were surprised that we did not detect hybridization with the *movo1* probe in the RNA preparation from adult ovary. The absence of hybridization could not be attributed to the quality of ovary RNA, since the glyceraldehyde-3-phosphate dehydrogenase (GAPDH) RNA control probe hybridized to a single, appropriately sized band. RT–PCR analysis revealed low levels of *movo1* transcripts in ovary and isolated mouse eggs (not shown). Whether *movo1* is more abundantly expressed in some transient developmental stage(s) or perhaps in a small

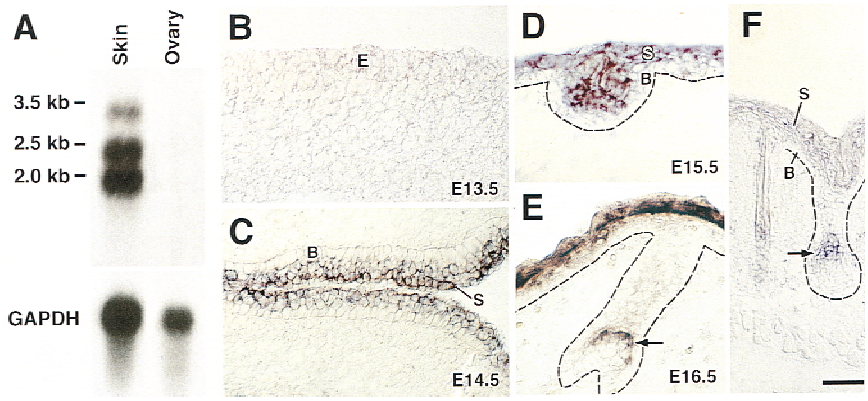

Figure 1. Examining *movo1* in skin and ovary. (*A*) Northern analysis of skin and ovary RNAs, loaded at 2 μg of polyA$^+$RNA per lane. Transcripts hybridizing with the *movo1* and GAPDH (control) probes are shown. (*B–E*) In situ hybridizations of digoxygenin-labeled *movo1* cRNA on embryonic skin from E13.5 to E16.5. In *C*, the developing epidermis at the embryo's arm–body junction is shown. (*F*) In situ hybridizations of *movo1* probe on newborn back skin. (E) Ectoderm; (S) suprabasal layers; (B) basal layer. Broken lines denote basement membrane. Arrows denote hybridizing signals in precortical cells of hair follicles. Bar, 50 μm in *B–E*; 80 μm in *F*.

population of cells within the ovary merits further investigation.

movo1 *mRNAs in differentiating cells of epidermis and hair follicle: in vivo and in vitro studies*

To examine *movo1* expression in more detail, we performed in situ hybridizations on skin from mouse embryos and neonatal mice. *movo1* mRNAs were first detected at embryonic day 14.5 (E14.5) in the suprabasal layers of developing epidermis (Fig. 1B,C). This is the earliest embryonic stage at which signs of epidermal differentiation are observed, with basal epidermal markers restricted to the innermost layer and early differentiation-specific markers appearing in suprabasal layers (Byrne et al. 1994).

By E15.5, *movo1* mRNAs could be seen in the inner cells of developing hair germs (Fig. 1D). As development proceeded, expression became restricted to inner root sheath and/or precortical cells of developing hair follicles (Fig. 1E,F, arrows). These cells will give rise to the hair shaft, i.e., the most terminally differentiated cells of the hair follicle.

Notably, *movo1* mRNAs were not detected in mitotically active epithelial cells of skin, including basal cells of epidermis, and matrix cells and outer root sheath of hair follicles. Thus, *movo1* expression occurred concomitantly with the onset of terminal differentiation in epidermis and its appendages. Intriguingly, the late-stage expression of *movo1* mRNAs correlated well with the fact that in *Drosophila*, *svb* function is manifested in cuticle-denticle formation, a differentiative process of epidermis that occurs well after the formation and patterning of the single-layered epithelium (Martinez Arias 1993).

To further explore the relationship between *movo1* and differentiation, we turned to mouse keratinocyte cultures, which upon elevating the levels of calcium, can be induced to undergo morphogenetic and molecular events resembling terminal differentiation (Hennings et al. 1980). When calcium is <0.05 mM, the mouse keratinocyte line UG1 behaves as a population of basal-like epidermal cells. RNAs isolated from these rapidly dividing cultures contained few transcripts that hybridized with a *movo1*-specific cDNA (Fig. 2). Within 24 hr after increasing calcium to 1.2 mM, a marked up-regulation of *movo1* RNAs was observed. Intriguingly, the appearance of *movo1* mRNAs preceded those of K1 encoding an early marker of terminal differentiation (Fuchs 1995).

The 30-kD mOvo1a protein concentrates in the nucleus of epithelial cells

Sequence similarities to known transcription factors and the nuclear localization of recombinant *Drosophila* Ovo fusion proteins have led to the hypothesis that *Drosophila* Ovo is a DNA-binding protein with transcriptional regulatory activity (Mevel-Ninio et al. 1991, 1995; Garfinkel et al. 1992; Lu et al. 1998). To test this possibility for mOvo1a, we engineered a vector to drive *movo1a* expression under the control of the cytomegalovirus (CMV) promoter. To detect the recombinant protein, we generated a polyclonal anti-mOvo1 antibody. When Cos monkey epithelial cells were transfected with the CMV–mOvo1a expression vector, a protein of 30 kD was produced, which by immunoblot analysis was detected by anti-mOvo1 (Fig. 3 A,B). This 30-kD protein was not produced by mock-transfected Cos cells, confirming its identity as mOvo1a.

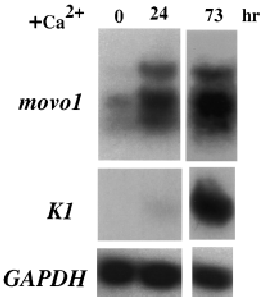

Figure 2. Northern analysis of RNAs isolated from mouse keratinocytes cultured in the presence of 1.2 mM Ca^{2+} for the hours (hr) indicated. Twenty micrograms of total RNAs was loaded in each lane. The same blot was stripped and rehybridized with the probes indicated.

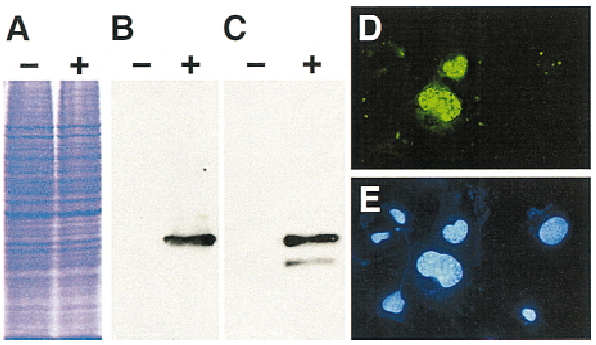

Figure 3. Nuclear localization of mOvo1a in transfected Cos cells. (*A*) Coomassie blue staining of SDS-PAGE-resolved proteins from Cos cells transfected with empty vector (−) or with CMV–*movo1a* (+). (*B*) Anti-mOvo1 immunoblot analysis of same extracts in *A*. Chemiluminescence was used to visualize the signal. Major band is at 30 kD. (*C*) Anti-mOvo1 immunoblot analysis of nuclear extracts prepared from Cos cells transfected as in *A*. Note: The minor ~25-kD band is a degradation product of the full-length protein as its presence in repeated experiments was variable. (*D*,*E*) Anti-mOvo1 (green) and DAPI (blue) immunofluorescence of Cos cells transfected with CMV–*movo1a*. Note: Anti-mOvo1 labeling restricted to the nuclei of transfected cells. Bar, 50 μm in *D* and *E*.

To determine mOvo1a's location, we repeated the transfection and immunoblot experiments, this time making nuclear extracts of CMV–mOvo1a and mock-transfected cells. As shown in Figure 3C, mOvo1a was detected in this nuclear fraction. Immunofluorescence localization confirmed that anti-mOvo1 recognized a nuclear protein restricted to the transfected cells (Fig. 3, D,E). In agreement with this result, we noted the presence of a putative nuclear localization signal (KKIHGVQQKYAYKERRA) at amino acid position 193 of the protein.

Analysis of the function(s) of nuclear mouse Ovo1 proteins must await a comprehensive analysis of the various mOvo1 isoforms and an exploration into their ability to regulate specific genes or processes involved in terminal differentiation. However, the existence of *Drosophila svb/ovo* and mouse *ovo1* transcripts in differentiating epidermis is intriguing and raises the possibility that conservation of transcriptional regulatory sequences may exist within the *ovo/svb* class of genes of different species.

Expression of movo1 *mRNAs in testis and kidney but not in many other tissues*

A more extensive analysis of tissues revealed *movo1* mRNAs in testis and kidney, and weakly in lung but absent in many other tissues (Fig. 4). As before, three hybridizing bands were detected, although their relative levels were somewhat different from those observed in skin. Interestingly, the tissue distribution of *movo1* mRNAs appeared to be distinct from that reported for *movo2*, which appeared to be restricted to testis, although skin was not examined (Masu et al. 1998). Whether there is an as yet unidentified mouse *ovo* gene that will be expressed in female germ-line development awaits future studies.

Generation of movo1$^{-/-}$ *mice*

Given the complexities of transcriptional regulation of the *ovo* genes in flies and mice, and the partially distinct expression patterns of the two known mouse *ovo* genes, we turned to a knockout strategy to examine the functional importance of mOvo1. Upon screening a 129/Sv mouse genomic library, two positive *movo1a*-hybridizing clones were identified. A partial restriction map of the *movo1* genomic DNA is shown in Figure 5A. The positioning of the exon–intron structure was determined by partial sequencing and is shown at the top of the figure. Southern blot analysis using several different probes detected only a single band, indicative of a single *movo1* gene (Fig. 5B–D; data not shown).

Because all of the *ovo* locus transcripts seem to encode the zinc finger domains, we designed a targeting vector to delete these sequences, contained entirely within exons 3 and 4 of the *movo1* gene (Fig. 5A). The 5.5- and 1.5-kb flanking *movo1* genomic fragments were used as 5′ and 3′ arms, respectively. The phosphoglycerate kinase 1 (PGK) promoter-driven neomycin-resistance gene was used for positive selection with G418, and the PGK promoter-driven herpes thymidine kinase (tk) gene was used for negative selection with Gancyclovir.

Of 130 R1 strain ES clones that survived in the presence of G418 and Gancyclovir, 11 scored positive for the homologous recombination event, as judged by Southern blot analysis (Fig. 5B,C). These clones were also examined using a radiolabeled probe corresponding to the neo gene to verify that no random integration of the vector had occurred elsewhere in the ES genome (not shown).

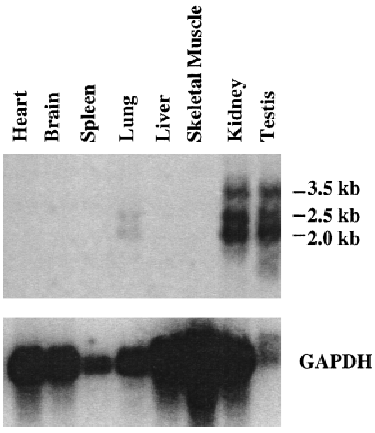

Figure 4. Tissue-specific expression of *movo1* RNAs. Poly(A)$^+$–RNAs were hybridized with a *movo1*-specific probe (*top*). The blot was then stripped and rehybridized with a GAPDH probe (*bottom*). The sizes of the three *movo1* transcripts are indicated at the *right*.

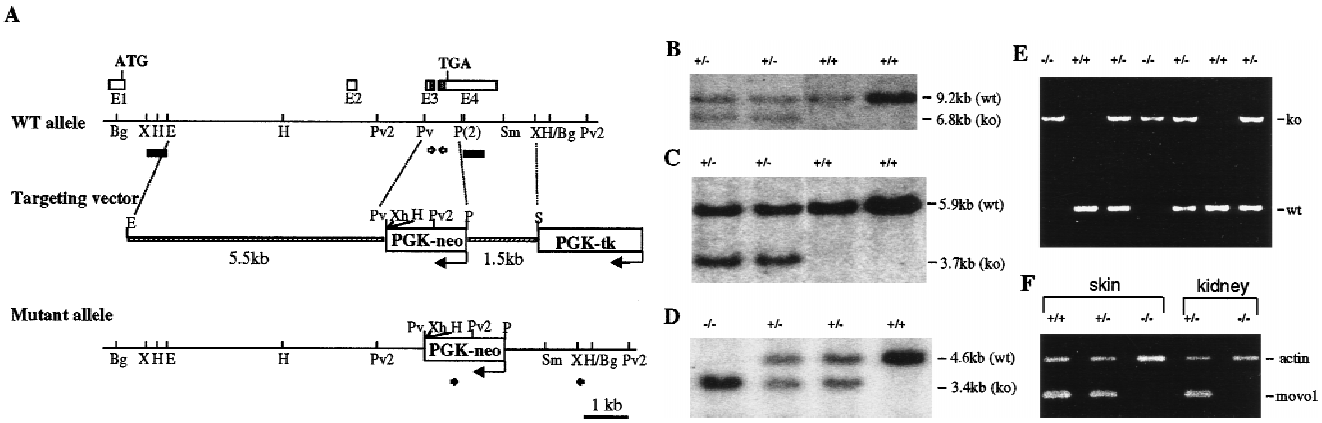

Figure 5. Disruption of *movo1* gene in ES cells and in mice. (*A*) Stick diagrams of the *movo1* locus (*top*), targeting vector (*middle*), and mutant locus resulting from homologous recombination (*bottom*). Exons (E1–E4) are shown as boxes above the wild-type allele. Translation initiation codon (ATG) and stop codon (TGA) are as indicated; shaded segments denote zinc finger domains. Black bars denote 5′ and 3′ probes used for Southern blot analysis; hatched boxes denote *movo1* sequences used for arms. (Bg) *Bgl*II; (X) *Xba*I; (H) *Hin*dIII; (E) *Eco*RI; (Pv2) *Pvu*II; (Pv) *Pvu*I; (P) *Pst*I; (S) *Sal*I; (Sm) *Sma*I; (Xh) *Xho*I. (*B–D*) Southern blot analyses of genomic DNAs from representative ES clones (*B*, 5′ probe; *C*, 3′ probe) and mouse tails (*D*, 3′ probe). DNAs were digested with *Xba*I–*Xho*I (*B*), *Hin*dIII (*C*), or *Pvu*II (*D*). (*E*) PCR analysis of genomic DNAs from mouse tails. The pair of primers denoted by black arrows in *A* generated a 2.5-kb product diagnostic for homologous recombination (ko band). The pair of primers denoted by white arrows in *A* generated a 330-bp product unique for the wild-type allele (wt band). (*F*) RT–PCR analysis of total RNAs isolated from skin and kidney of $movo1^{+/+}$, $movo1^{+/-}$, and $movo1^{-/-}$ mice. Set of primers used generated a band corresponding to the targeted zinc finger domains of *movo1*. Actin primers were used as an internal control.

Two of these clones were used to generate $movo1^{-/-}$ mice. Both contributed to the germ line, as verified by Southern blot and PCR analysis of mouse tail DNAs (Fig. 5D,E).

To examine the outcome of *movo1* RNA synthesis in the mutant mice, we used primers specific for sequences within the zinc finger region for RT–PCR analysis. A fragment of the expected size was generated in skin and kidney RNAs from wild-type (+/+) and heterozygous (+/−)mice, but not from homozygous $movo1^{-/-}$ mice (Fig. 5F). By Northern blot analysis, some large transcripts were generated from the mutated locus, as is often typical in gene targeting events. However, the two most abundantly expressed transcripts in wild-type skin were absent from homozygous $movo1^{-/-}$ skin RNAs (not shown). Thus, it is likely that the *movo1* locus was functionally inactivated as a consequence of the targeting event.

movo1$^{-/-}$ *skin morphology is largely normal, but mice have a ruffled hair coat and hair abnormalities*

At the light microscopy level, no obvious morphological differences were observed in epidermis or its appendages (Fig. 6). Additionally, expression and activity of suprabasal markers of terminal differentiation appeared normal (for review, see Fuchs 1995). Our analysis included (1) involucrin and K1 expressed early in epidermal differentiation; (2) filaggrin and loricrin expressed at later stages of epidermal differentiation; (3) transglutaminase activated late in epidermal and hair follicle differentiation upon an influx in intracellular calcium pools; and (4) hair-specific keratins and cuticle/inner root sheath-specific trichohyalin (for representative examples, see Fig.

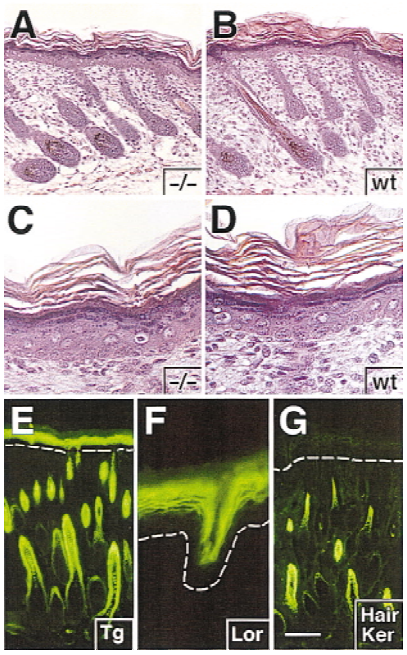

Figure 6. Morphology and biochemistry of $movo1^{-/-}$ back skin. Back skins of a newborn $movo1^{-/-}$ mouse and control littermate (wt) were processed for histology and immuofluorescence microscopy. (*A–D*) Hematoxylin- and eosin-stained sections. (*E*) Immunofluorescence assay for transglutaminase (Tg) activity in $movo1^{-/-}$ back skin. (*F,G*) Immunofluorescence staining of $movo1^{-/-}$ back skin with antibodies to loricrin (Lor, *F*) and hair keratins (hair ker, *G*). Immuofluorescence patterns were indistinguishable from wild type (not shown). Broken lines denote basement membrane. Bar, 160 μm in *A* and *B*; 40 μm in *C* and *D*; 110 μm in *E* and *G*; 30 μm in *F*.

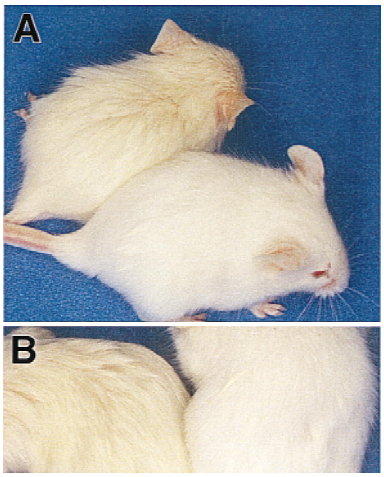

Figure 7. Aberrant hair coat of the *movo1*$^{-/-}$ mice. (*A*) *movo1*$^{-/-}$ mouse (*top*) and control littermate (*bottom*). (*B*) Close-up of the back area from mutant (*left*) and control (*right*) mice.

6E–G). In all of these cases, the *movo1*$^{-/-}$ skin was indistinguishable from wild type.

Whereas no obvious biochemical abnormalities were detected with the epidermal and hair-specific markers that we examined, the *movo1* mice nevertheless began to develop aberrations in their hair coat that were visible to the eye by the age of about two weeks (Fig. 7). By this time, *movo1*$^{-/-}$ mutant mice were distinguished from control littermates by their fuzzy, ruffled hair coat. This phenotype was somewhat more prominent in males, but was seen in both sexes. In addition, the *movo1*$^{-/-}$ mice were runted: On average, adult (−/−) mice weighed ~20%–25% less than littermates.

Scanning electron microscopy revealed structural abnormalities in the hairs of *movo1*$^{-/-}$ mice even at early ages (Fig. 8). A number of hairs displayed kinks and/or intercellular splits within or along the hair shafts. Such splits were predominantly seen in guard hairs, the longest and straightest of the four hair types (Dry 1926). Light microscopic examination of at least 50 plucked hairs from each type (~1000 hairs in total) confirmed that 16% of the guard hairs exhibited some signs of separation or splitting. Occasional auchene or awl hairs were also defective. In contrast, hairs plucked from control littermates showed no splits or alterations in any of the four hair types.

The abnormalities in the hairs seemed to arise from a structural weakness or subtle change in the intercellular interactions within the hair shaft. However, at the ultrastructural level, we saw no obvious changes within the cells of the inner root sheath, outer root sheath, cuticle, cortex, or medulla (not shown). The restriction of aberrations to late-stage differentiation within the hair shaft is consistent with *movo1* gene expression in the precortical cells of wild-type follicles. Precisely how *movo1* expression might influence these intercellular interactions in the hair shaft awaits the identification and characterization of the genes regulated by mOvo1.

Defects in the kidney and urogenital system of movo1$^{-/-}$ *mice*

In situ hybridization revealed that *movo1* RNAs in the wild-type kidney localize to the renal tubules of cortex and not to the glomeruli (Fig. 9, A, antisense; B, sense). In *movo1*$^{-/-}$ kidneys, defects were detected as early as 6 days postnatally; small cysts appeared within the developing cortex (Fig. 9C). The number and size of these epithelial cysts increased with age (Fig. 9E). In addition to these histological anomalies in the kidney, focal cystic dilation was sometimes observed in adult kidneys with accompanying signs of atrophy of surrounding renal tubules and glomeruli (not shown). Given their late onset, these changes are likely to be secondary consequences either from cyst formation within the kidney and/or from a defective urogenital system (see below).

Urogenital defects were particularly striking in female *movo1*$^{-/-}$ mice. Approximately 60% of adult female *movo1*$^{-/-}$ mice exhibited visibly moist skin in the external area surrounding the urogenital tract. This became so severe that in some cases, hair loss occurred in this region. When dissected and examined, these female mutants consistently showed a markedly dilated uterus and cervix, with some degeneration of the epithelial lining of the lumen (not shown). In addition, the external vaginal opening was often constricted and in a few cases, completely fused (data not shown). At present, we do not yet know how mOvo1 might function to control such pro-

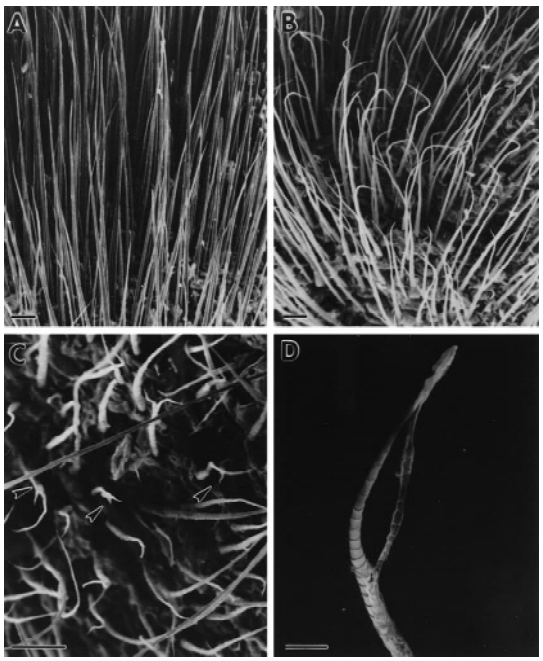

Figure 8. Scanning electron microscopy of skin surface from *movo1* mutant and control mice. Back skins are from similar regions of an 8-day-old mutant mouse (*B*,*C*) and control littermate (*A*). Arrowheads in *C* denote splits at the hair ends. (*D*) Higher magnification of a mutant hair from the *movo1* mouse to reveal intercellular nature of the split. Bar, 100 µm in *A*–*C*; 10 µm in *D*.

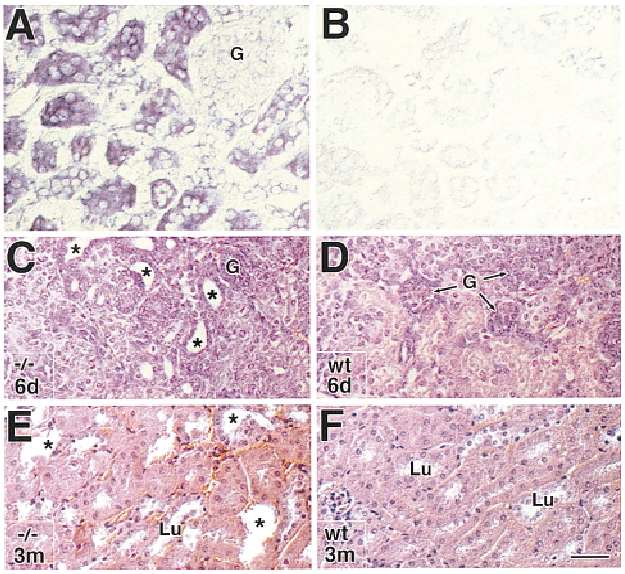

Figure 9. *movo1* expression in kidney and effect of *movo1* ablation on kidney morphology. (*A*,*B*) In situ hybridizations of *movo1* (*A*) or sense (*B*) probe on frozen sections of adult kidney. Note hybridizing signals in kidney tubules but not in glomeruli (G). (*C*,*D*) Kidneys from a 6-day-old mutant mouse (*C*) and littermate (*D*). (*E*,*F*) Kidneys from a 3-month-old mutant mouse (*E*) and littermate (*F*). Asterisks (*) denote cysts in mutant kidneys not to be confused with tubule lumens (Lu). Bar, 75 μm.

cesses. This said, it is curious that whereas hair defects were more prominent in males, urogenital defects occurred predominantly in females. The possible relation between these sex-related alterations in mouse and the sex-related functions of *ovo* in flies awaits further investigation.

Cases of imperforate vagina can occur at a frequency of up to 10% in some laboratory mouse strains (Sundberg and Brown 1994). However, none of the control littermates in our study displayed urogenital defects under conditions in which 60% of female *movo1* mutant mice did so. These data argue that the observed structural malformations resulted from genetic manipulation of the *movo1* locus. These alterations affected the mating ability of females; however, even when these mice were stimulated with hormone, superovulation resulted in normal numbers of eggs (data not shown).

movo1-*related defects in late stage spermatogenesis*

In situ hybridizations of wild-type mature testis detected *movo1* RNAs in primary and secondary spermatocytes, but not in spermatogonia (Fig. 10). These findings were interesting in that (1) *Drosophila ovo/svb* transcripts occur early, and not late, in male germ-cell development (Oliver et al. 1994; Mevel-Ninio et al. 1995); and (2) *movo2* transcripts are expressed in testis only 3 weeks postnatally, that is, at a time when spermatogonia have given rise to spermatocytes (Masu et al. 1998). Taken together, these findings suggest an evolutionary difference in transcriptional regulation of the *ovo/svb* class of genes in the male germ line, and a role for *movo* expression in late-stage differentiation of male germ cells.

Morphological defects in *movo1* mutant testes correlated with the timing of *movo1* expression in wild-type mice. During the first few weeks postnatally, testes appeared normal in size and morphology (Fig. 11, A and B, mutant vs. wild type). In contrast, by 4 weeks, testes were abnormally small: After correction for the overall reduction in body weight of the $movo1^{-/-}$ male mice, mutant testes were only 15%–50% the weight of normal testes (see Fig. 11C for intermediate example).

Two types of testis-related morphological defects were detected. In the 1-month-old mutant testis, the diameters of seminiferous tubules and the numbers of cells within tubules were atypically small (Fig. 11, D and E, respectively). Because testis size was not affected in younger animals, we surmise that this reduction is a reflection of a failure of germ-cell maturation and/or survival. Consistent with this notion was a marked reduction in the number of mature spermatids that reached the lumen. Interestingly, a lack of vascularization was seen in the mutant testes (Fig. 11C), as was also the case for mutant kidneys (not shown).

Additionally, seminiferous tubules of older mutant mice showed signs of degeneration (Fig. 11F,H,J,K). Differentiating cells from the primary spermatocyte stage onward appeared defective. In severely affected testes, only a few spermatogonia survived (see Fig. 11K, arrowheads), and often Sertoli cells were the only remnants of the tubules (Fig. 11H). Because defects in germ-cell survival were not detected early in postnatal testis development, we surmise that they developed over time, perhaps as a secondary consequence of defective sperm production.

Despite defects in many seminiferous tubules, some produced sperm (Fig. 11J,K). Moreover, whereas sperm production was greatly diminished, male *movo1* mutant mice were not completely sterile.

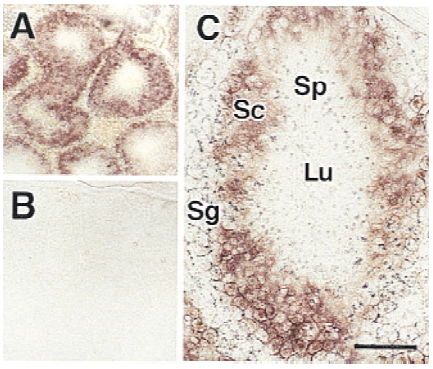

Figure 10. *movo1* RNA expression in testis. In situ hybridizations of *movo1* (*A* and *C*) or sense (*B*) probes on frozen sections of adult testis. Note hybridization in germ cells of seminiferous tubules. Hybridization was not detected in spermatogonia (Sg), but was prominent in spermatocytes (Sc). (Lu) Lumen; (Sp) spermatids. Bar, 60 μm in *C*; 200 μm in *A* and *B*.

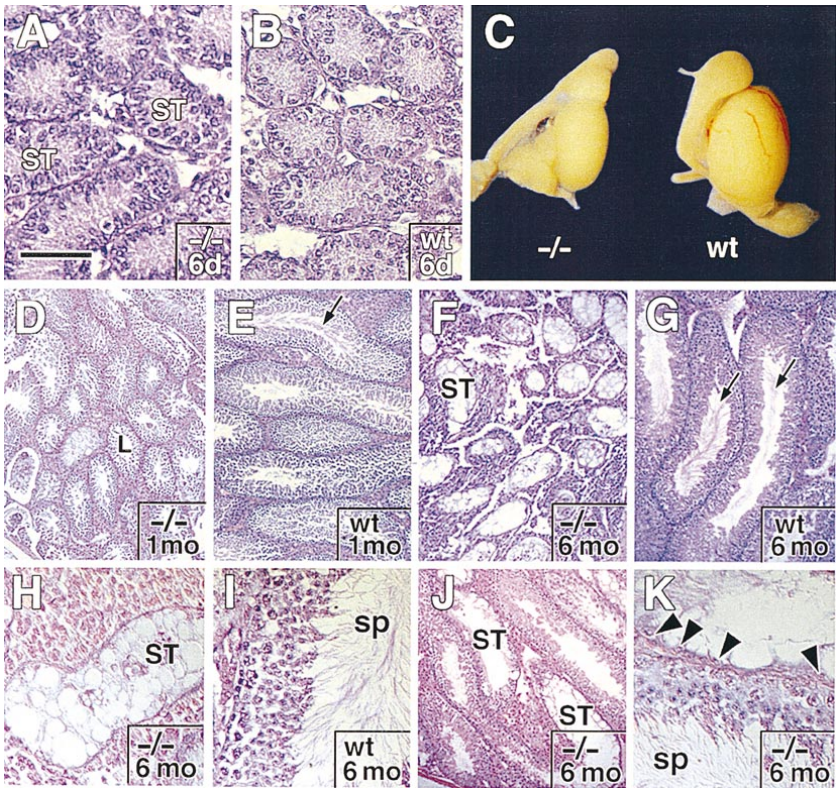

Figure 11. Morphological abnormalities in the *movo1* mutant testes. Shown are hematoxylin- and eosin-stained sections of representative testes from *movo1*$^{-/-}$ mice and control littermates (wt) at ages indicated. Whole testes are from 1-month-old mice; corresponding sections of these tissues reveal a dramatic difference in the size of the developing seminiferous tubules (*D* and *E* are at same magnification). Note the presence of sperm (arrows, SP) in lumen of mature wild-type, but not in most mutant, seminiferous tubules (ST). (*K*) Section of testis from mutant mouse that fathered five litters. The upper tubule was typical of *movo1*$^{-/-}$ testes: Arrowheads denote a few spermatogonia left in an otherwise degenerated seminiferous tubule; often only Sertoli cells remained. *movo1*$^{-/-}$ tubule in lower part of frame *K* displayed normal-looking sperm. Bar, 55 µm in *A* and *B*; 6.5 mm in *C*; 280 µm in *D* and *E*; 240 µm in *F*, *G*, and *J*; 60 µm in *K*.

Discussion

Similarities between fly and mouse epidermis

Fly larval epidermis is composed of a single layer of cells that secret a proteinaceous, extracellular cuticle (Fig. 12A). It also makes appendages such as ventral denticles and dorsal hairs, presumably providing sensory and locomotor functions. Cuticular appendage morphogenesis entails the transient formation of filopodia-like protrusions supported by the epidermal cell's cytoskeleton; following cuticle secretion and hardening, these extensions retract, leaving a hardened, appendage-like structure at the fly's body surface (Martinez Arias 1993; Dickinson and Thatcher 1997).

In contrast, higher vertebrates display a stratified epidermis whose layers differ in proliferative capacity and differentiation status (Fig. 12B). Within the innermost, basal epidermal layer, a small stem cell population gives rise to transiently dividing cells with a limited proliferative capacity. Periodically, one of these cells withdraws from the cell cycle and commits to terminal differentiation. As the cell moves outward, it changes its program of gene expression to tailor a tough, resilient cytoskeleton. In this way, the protective material shed from the skin surface is cellular rather than secreted (Fuchs 1995). The major mammalian epidermal appendage is the hair follicle, which again is cellular, rather than extracellular (Hardy 1992).

As distinct as epidermal morphogenesis may appear in these evolutionarily distant animals, some parallels still remain. Whether in fly or mouse, the epidermis must provide a protective armor to keep microorganisms out and essential bodily fluids in. In both species, the epidermis manifests this function by producing a single-layered epithelium that can execute a differentiative process. Whether secretory or cellular, surface appendages in both species are produced by epidermis late in embryogenesis (Hardy 1992; Martinez Arias 1993; Fuchs 1995). Even though the major structural genes of fly (cuticle) and mice (keratin) are not related, several of the genetic pathways that govern the patterning of appendages may be conserved (Parr and McMahon 1995; Willert and Nusse 1997), a notion underscored by the recent discovery that mutations in the human *patched* gene, first identified as a fly epidermal gene, are responsible for basal-cell carcinomas (Hahn et al. 1996; Johnson et al. 1996).

Our studies on *movo1* coupled with prior studies on *ovo/svb* (Oliver et al. 1987; Mevel-Ninio et al. 1991) now suggest that genetic parallels between fly and mouse epidermis go beyond the patterning of their appendages to the genes that are involved in structural aspects of epidermal differentiation and/or appendage formation. Thus, the *ovo/svb* class of genes encodes proteins with four evolutionarily conserved Cys_2–His_2 zinc-finger motifs that are involved in regulating cuticle/denticle formation in flies and hair differentiation in mice, both processes that occur late in differentiation. When taken together with evidence that Ovo/Svb are nuclear DNA-binding proteins (Mevel-Ninio et al. 1994; Lu et al. 1998), we anticipate that there will be downstream target genes for *movo1*-encoded proteins that are involved in termi-

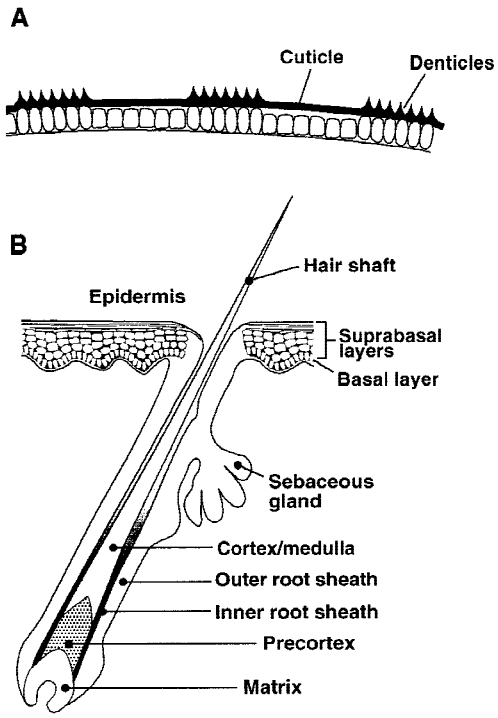

Figure 12. Schematic diagram of the fly and mouse epidermis. (*A*) Fly larval epidermis is composed of a single layer of cells. These cells are arranged in a specific spatial pattern such that those that make denticles alternate with those that do not. Denticle formation occurs late in larval development, and stems from epithelial protrusions, hardened by cuticle secretion. (*B*) Mouse epidermis and hair follicles arise from a single-layered embryonic ectoderm. In the adult, the epidermis is composed of a single layer of mitotically active basal cells and multiple layers of terminally differentiating suprabasal cells. The hair follicle is more complex. The cellular hair shaft arises from upward differentiation of matrix cells into precortex cells and finally into the cortex and medulla. It is encased by two cellular root sheaths, the outermost of which is contiguous with the epidermis.

nal differentiation in hair, and possibly in epidermis, in which *movo1* is also expressed.

mOvo and spermatogenesis

In *Drosophila*, *ovo* is expressed in all germ cells, but its only function appears to be in female germ cells, where it is required for female sex determination and oogenesis (Comer et al. 1992; Oliver et al. 1994; Mevel-Ninio et al. 1995). In contrast, *movo* genes seem to have evolved to play a role in mammalian spermatogenesis. This is perhaps not surprising given that in mammals, the default pathway for germ-line sex determination has changed from male to female, and sex determination has evolved to differ quite dramatically from *Drosophila* (for review, see Pauli and Mahowald 1990; McLaren 1995). In mice, *movo1* does not appear to be required for sex determination, because at least some viable male and female homozygous mutant *movo1* germ cells develop, resulting in a few successful matings of homozygous *movo1*$^{-/-}$ mice within the population.

The defects in *movo1* mutant testes occurred late, concomitant with the late onset of *movo1* expression in the testis. Interestingly, despite the lack of appreciable *movo1* expression in spermatogonia, male germ-line stem-cell survival was also affected, a process that coincided with major signs of tubule degeneration in adult animals. At present, we surmise that the defects in sperm production are primary, whereas those in male germ-cell survival and in testis vascularization are secondary. Regardless of the sequence of events, the degeneration seen in the mutant testes was among the most striking of the defects caused by *movo1* mutation.

Abnormalities in the kidneys and urogenital tract of movo1 *mutant mice*

Given the phenotype of *ovo/svb* mutant flies, we had not anticipated defects in the kidney and urogenital tract of our *movo1* mutant mice. However, it is interesting and likely relevant that the ovary, testis, and kidney share a common embryonic origin. These organs are derived predominantly from intermediate mesoderm, which undergoes extensive epithelial transformation to generate the ducts and tubules that compose urogenital tracts and kidneys (for review, see Saxen 1987). The tubule degeneration seen in the kidneys of our mice was similar to that seen in the testes. Our findings suggest that *ovo/svb* class of genes function in the differentiation and/or maintenance of the urogenital system.

A number of other transcription factors have been shown to govern the development of the urogenital system (Pelletier et al. 1991; Satokata et al. 1995; Torres et al. 1995; Miyamoto et al. 1997). In particular, Pax2 seems to be essential in the early development of these structures, as *Pax2* mutant mice lack kidneys, ureters, and genital tracts (Torres et al. 1995). In contrast, *movo1* mutant mice seem to develop all of these structures normally but exhibit late-stage defects in the differentiation and/or maintenance of the kidneys and testes. As in the *Pax2* mutant mouse, related endoderm-derived components, such as the bladder, urethra, and prostatic glands appear to be unaffected in *movo1* mutant mice.

The existence of at least two ovo/svb *genes in mice: functional redundancy or differential functions?*

Given the existence of multiple *movo* genes (Masu et al. 1998), *ovo/svb* function may be even more important than what our *movo1* mutant mice suggest. If the products of the different mouse *ovo/svb*-like genes share similar functions, then a threshold level of the encoded protein could be necessary to properly manifest normal differentiative functions in the organs where these genes are expressed. Alternatively, it could be that functions stemming from the *ovo/svb* locus in flies have evolved and diverged through gene duplication. In this fashion, we might expect that *movo2* and other as yet unidenti-

fied mouse *ovo* genes may encode Ovo/Svb-like proteins with distinct functions. Distinguishing between these possibilities must await future ablation of other *movo* genes and characterization of the multiple *movo* transcripts and their proteins.

Do ovo *genes play a role in human disease?*

The fact that *movo1* mutant mice survive to adulthood and are not completely infertile raises the possibility that mutations in the equivalent human gene might give rise to a complex disorder involving hypogonadism, renal and urogenital defects, and mild hair abnormalities. Using FISH technology, we mapped the mouse *ovo1* gene to a region of chromosome 19 close to the centromere (J. Fantes, C. Schonbaum, and X. Dai, unpubl.). The equivalent region in the human genome is chromosome 11q13, where the human *ovo1* gene was recently shown to reside (Chidambaram et al. 1997). Intriguingly, chromosomal rearrangements involving 11q13 have been observed in extragonadal germ-cell tumors (Sinke et al. 1994) and in renal oncocytomas (van den Berg 1995). In addition, the genetic disorder Bardet–Biedl syndrome maps to this locus (Leppert et al. 1994; Beales et al. 1997). This syndrome encompasses certain traits, such as mental retardation, post-axial polydactylia, obesity, and pigmentary retinopathy, that are inconsistent with those of the *movo1* mutant mice. However, some Bardet–Biedl syndrome patients exhibit hypogenitalism in males, vaginal anomalies in females, and kidney/urogenital abnormalities (Leppert et al. 1994; Carmi et al. 1995; O'Dea et al. 1996; Beales et al. 1997). These traits are strikingly consistent with the defects seen in our *movo1* mutant mice. Whereas the pleiotropic phenotypes associated with this syndrome seem to extend beyond those that can be accounted for by *ovo1*, the complex nature of the *ovo* genes and the partial overlap in phenotypic traits between our mice and Bardet–Biedl syndrome leave open the possibility that the *ovo1* gene may be involved in this or perhaps other syndromes involving abnormalities of the urogenital system.

Materials and methods

Northern analysis

Total skin RNAs were isolated from frozen and powdered skin using the TRIzol reagent from GIBCO-BRL (Gaithersburg, MD). Poly(A)$^+$-RNAs were isolated using Oligotex (Qiagen, Valencia, CA).Ovary poly(A)$^+$-RNAs were purchased from Ambion (Austin, TX). Northern blots containing other adult mouse tissues were purchased from Clontech (Palo Alto, CA). One of the following probes was used: a 1.0-kb fragment containing the 5′-end sequences of the *movo1* cDNA including all four zinc fingers; a 350-bp fragment containing mostly 5′ UTR of *movo1*; or a 1.2-kb fragment containg the 3′ UTR and part of the coding sequences including three of the four zinc fingers. All three probes gave rise to similar results. Hybridizations were performed in ExpressHyb hybridization solution from Clontech at 68°C, followed by two washes in 2× SSC, 0.05% SDS at room temperature, and three washes with 0.1× SSC, 0.1% SDS at 65°C.

In situ hybridization and immunofluorescence

In situ hybridizations with digoxygenin-labeled cRNA probes were performed on frozen sections using the method of Schaeren-Wiemers and Gerfin-Moser (1993) with slight modifications: 10% heat-inactivated goat serum was used as the blocking agent prior to incubation with anti-digoxygenin antibody. Two different probes were used and yielded similar results: a 1.0-kb cRNA containing the four zinc fingers and upstream sequences; a 870-b cRNA containing the 3′ UTR of *movo1*.

Immunofluorescence microscopy was performed as described (Allen et al. 1996). A rabbit polyclonal antibody was generated by Zymed Laboratories (San Francisco, CA) to the peptide sequence CTSESQEGHVLHLKERHPDS at amino acid position 220 of mOvo1a protein. Antiserum was affinity purified on a peptide-conjugated column using the Sulfolink kit (Pierce, Rockford, IL) according to manufacturer's suggestions. Rabbit anti-loricrin was raised in the laboratory (E. Fuchs, K. Turksen, and L. Milstone, unpubl.). AE13 was kindly provided by T.-T. Sun (New York University School of Medicine, NY).

Transglutaminase assay

Transglutaminase activity was measured using the following procedure. Frozen skin sections were fixed in methanol (−20°C) for 20 min, followed by 2 × 5-min washes in PBS. Sections were then incubated with a solution containing 2.5 mM DTT, 0.25% Triton X100, 0.15 M NaCl, 0.05 M Tris-HCl at pH 8.0, 10 mM $CaCl_2$, and 20% dansyl cadaverine, washed 3 × 5 min in PBS, and mounted as described (Allen et al. 1996). Transglutaminase activity was then detected by fluorescence microscopy.

Cell culture and transient transfections

Mouse keratinocyte line UG1 (spontaneously immortalized and cloned by Uri Gat in the laboratory) were cultured in media containing <0.05 mM Ca^{2+} (Hennings et al. 1980). In Ca^{2+} induction experiments, $CaCl_2$ was added to the subconfluent culture at a final concentration of 1.2 mM, and cells were then maintained in high Ca^{2+} for desired period of time before harvesting. Full-length 2.0-kb *movo1a* cDNA was released from the Bluescript vector by *Eco*RI–*Asp*I restriction and cloned into the *Kpn*I site of the mammalian expression vector pCB6(+) containing a CMV promoter and enhancer. Cos cells were transfected with the resulting plasmid using the calcium-phosphate method (Wigler et al. 1978).

Generation of movo1$^{-/-}$ *mice*

Full-length *movo1* cDNA was used to screen a 129/Sv genomic library. One resulting clone was subjected to detailed restriction map analysis and used to construct the targeting vector. The targeting vector was electroporated into R1 ES cells (passage 12) at 270 V, 500 μF in a GenePulser (Bio-Rad Laboratories, Hercules, CA). ES cell culture and drug selection was essentially as described (Lo et al. 1997). ES clones positive for desired homologous recombination were injected into C57BL/6 blastocyst, and the resulting chimeric mice were crossed with C57BL/6. Germline transmission was obtained with two ES clones. Southern blot or PCR analysis was used for genotyping the ES clones and the mutant mice. For Southern blot analysis, genomic DNA was digested with *Xba*I–*Xho*I, *Hin*dIII, or *Pvu*II, run on a 0.7% agarose gel, transferred to positively charged nylon membrane, and hybridized with either a 5′ (1.0-kb *Xba*I–*Eco*RI fragment) or a 3′ (1.5-kb *Pst*I–*Xba*I fragment) probe.

Histology

Tissues were fixed in Bouin's fixative or in 4% formaldehyde, processed, and embedded in paraffin. Sections (5 µm) were stained with hematoxylin and eosin, examined, and photographed using an Axiophot microscope (Carl Zeiss, Thornwood, NY).

Electron microscopy

Electron microscopic (EM) studies were kindly assisted by Edward Williamson at the Cancer Research Center EM facility of the University of Chicago, Illinois. For scanning EM, back skins of 8-day-old mutant mice and littermates were control fixed, processed, and examined as described (Guo et al. 1996).

Acknowledgments

We thank Janet Rossant and Andras Nagy at Mount Sinai Hospital, Toronto, for kindly providing us with R1 strain ES cells. We thank Su Hao Lo and Liz Allen for their help and advice with the mouse work. We are grateful to Ed Williamson for his expert help at the EM facility, to Christoph Bauer and Mei Yin for their help in printing the EM pictures, and Chuck Wellek for his help in assembling the computer images for the figures. This work was supported by a grant from the National Institutes of Health (NIH) (AR31737). X.D. is the recipient of a postdoctoral fellowship from NIH (5 F32 AR08456-03). E.F. is an Investigator of the Howard Hughes Medical Institute.

The publication costs of this article were defrayed in part by payment of page charges. This article must therefore be hereby marked 'advertisement' in accordance with 18 USC section 1734 solely to indicate this fact.

References

Allen, E., Q.-C. Yu, and E. Fuchs. 1996. Abnormalities in desmosomes, proliferation and differentiation in the epidermis of mice expressing a mutant desmosomal cadherin. *J. Cell Biol.* **133:** 1367–1382.

Andrews, J., I. Levenson, and B. Oliver. 1998. New AUG initiation codons in a long 5′ UTR create four dominant negative alleles of the *Drosophila* C2H2 zinc-finger gene *ovo*. *Dev. Genes Evol.* **207:** 482–487.

Beales, P.L., A.M. Warner, G.A. Hitman, R. Thakker, and F.A. Flinter. 1997. Bardet-Biedl syndrome: A molecular and phenotypic study of 18 families. *J. Med. Genet.* **34:** 92–98.

Bogan, J.S. and D.C. Page. 1994. Ovary? Testis?—A mammalian dilemma. *Cell* **76:** 603–607.

Busson, D., M. Gans, K. Komitopoulou, and M. Masson. 1983. Genetic analysis of three dominant female sterile mutations located on the X-chromosome of *Drosophila melanogaster*. *Genetics* **105:** 309–325.

Byrne, C., M. Tainsky, and E. Fuchs. 1994. Programming gene expression in developing epidermis. *Development* **120:** 2369–2383.

Capel, B. 1998. Sex in the 90s: SRY and the switch to the male pathway. *Annu. Rev. Physiol.* **60:** 497–523.

Carmi, R., K. Elbedour, E.M. Stone, and V.C. Sheffield. 1995. Phenotypic differences among patients with Bardet-Biedl syndrome linked to three different chromosome loci. *Am. J. Med. Genet.* **59:** 199–203.

Chidambaram, A., R. Allikmets, S. Chandrasekarappa, S.C. Guru, W. Modi, B. Gerrard, and M. Dean. 1997. Characterization of a human homolog (OVOL1) of the *Drosophila ovo* gene, which maps to chromosome 11q13. *Mamm. Genome* **8:** 950–951.

Cline, T.W. and B.J. Meyer. 1996. Vive la difference: Males vs. females in flies vs. worms. *Annu. Rev. Genet.* **30:** 637–702.

Comer, A.R., L.L. Searles, and L.J. Kalfayan. 1992. Identification of a genomic DNA fragment containing the *Drosophila melanogaster* ovarian tumor gene (*otu*) and localization of regions governing its expression. *Gene* **118:** 171–179.

Dickinson, W.J. and J.W. Thatcher. 1997. Morphogenesis of denticles and hairs in *Drosophila* embryos: Involvement of actin-associated proteins that also affect adult structures. *Cell Motil. Cytoskel.* **38:** 9–21.

Dry, F.W. 1926. The coat of the mouse (Mus musculus). *J. Genet.* **16:** 287–340.

Fuchs, E. 1995. Keratins and the skin [Review]. *Annu. Rev. Cell Devel. Biol.* **11:** 123–153.

Garfinkel, M.D., A.R. Lohe, and A.P. Mahowald. 1992. Molecular genetics of the *Drosophila melanogaster ovo* locus, a gene required for sex determination of germline cells. *Genetics* **130:** 791–803.

Garfinkel, M.D., J. Wang, Y. Liang, and A.P. Mahowald. 1994. Multiple products from the *shavenbaby-ovo* region of *Drosophila melanogaster*: Relationship to genetic complexity. *Mol. Cell Biol.* **14:** 6809–6818.

Granadino, B., P. Santamaria, and L. Sanchez. 1993. Sex determination in the germline of *Drosophila melanogaster*: Activation of the gene Sex-lethal. *Development* **118:** 813–816.

Guo, L., L. Degenstein, and E. Fuchs. 1996. Ablation of keratinocyte growth factor in mice: Skin changes but no aberrancies in wound-healing. *Genes & Dev.* **10:** 165–175.

Hahn, H., C. Wicking, P.G. Zaphiropoulos, M.R. Gailani, S. Shanley, A. Chidambaram, I. Vorechovshky, E. Holmberg, A.B. Unden, S. Gillies et al. 1996. Mutations of the human homolog of *Drosophila patched* in the nevoid basal cell carcinoma syndrome. *Cell* **85:** 841–851.

Hardy, M.H. 1992. The secret life of the hair follicle. *Trends Genet.* **8:** 159–166.

Hennings, H., D. Michael, C. Cheng, P.M. Steinert, K. Holbrook, and S.H. Yuspa. 1980. Calcium regulation of growth and differentiation of mouse epidermal cells in culture. *Cell* **29:** 245–254.

Hillier, L., N. Clark, T. Dubuque, K. Elliston, M. Hawkins, M. Holman, M. Hultman, T. Kucaba, M. Le, G. Lennon et al. 1996. Washington University–Merck EST Project. mouseest@watson.wustl.edu.

Johnson, R.L., A.L. Rothman, J. Xie, L.V. Goodrich, J.W. Bare, J.M. Bonifas, A.G. Quinn, R.M. Myers, D.R. Cox, E.H. Epstein, Jr., and M.P. Scott. 1996. Human homolog of *patched*, a candidate gene for basal cell nevus syndrome. *Science* **272:** 1668–1671.

Leppert, M., L. Baird, K.L. Anderson, B. Otterud, J.R. Lupski, and R.A. Lewis. 1994. Bardet-Biedl syndrome is linked to DNA markers on chromosome 11q and is genetically heterogeneous. *Nat. Genet.* **7:** 108–112.

Lin, H. 1997. The tao of stem cells in the germline. *Ann. Rev. Genet.* **31:** 455–491.

Lo, S.H., Q.C. Yu, L. Degenstein, L.B. Chen, and E. Fuchs. 1997. Progressive kidney degeneration in mice lacking tensin. *J. Cell Biol.* **136:** 1349–1361.

Lu, J., J. Andrews, D. Pauli, and B. Oliver. 1998. *Drosophila* OVO zinc-finger protein regulates *ovo* and *ovarian tumor* target promoters. *Dev. Genes Evol.* **208:** 213–222.

Martinez Arias, A. 1993. Development and patterning of the larval epidermis of *Drosophila*. In *The development of Drosophila melanogaster* (ed. M. Bate and A. Martinez Arias),

pp. 517–608. Cold Spring Harbor Laboratory Press, Cold Spring Harbor, NY.

Masu, Y., S. Ikeda, E. Okuda-Ashitaka, E. Sato, and S. Ito. 1998. Expression of murine novel zinc finger proteins highly homologous to *Drosophila ovo* gene product in testis. *FEBS Lett.* **421:** 224–228.

McLaren, A. 1995. Germ cells and germ cell sex. *Phil. Trans. Roy. Soc. London-Series B: Biol. Sci.* **350:** 229–233.

Mevel-Ninio, M., R. Terracol , and F.C. Kafatos. 1991. The *ovo* gene of *Drosophila* encodes a zinc finger protein required for female germline development. *EMBO J.* **10:** 2259–2266.

Mevel-Ninio, M., R. Terracol, C. Salles, A. Vincent, and F. Payre. 1995. *Ovo*, a *Drosophila* gene required for ovarian development, is specifically expressed in the germline and shares most of its coding sequences with *shavenbaby*, a gene involved in embryo patterning. *Mech. Dev.* **49:** 83–95.

Mevel-Ninio, M., E. Fouilloux, I. Guena, and A. Vincent. 1996. The three dominant female-sterile mutations of the *Drosophila ovo* gene are point mutations that create new translation-initiator AUG codons. *Development* **122:** 4131–4138.

Miyamoto, N., M. Yoshida, S. Kuratani, I. Matsuo, and S. Aizawa. 1997. Defects of urogenital development in mice lacking Emx2. *Development* **124:** 1653–1664.

O'Dea, D., P.S. Parfrey, J.D. Harnett, D. Hefferton, B.C. Cramer, and J. Green. 1996. The importance of renal impairment in the natural history of Bardet-Biedl syndrome. *Am. J. Kid. Dis.* **27:** 776–783.

Oliver, B., N. Perrimon, and A.P. Mahowald. 1987. The *ovo* locus is required for sex-specific germ line maintenance in *Drosophila. Genes & Dev.* **1:** 913–923.

Oliver, B., D. Pauli, and A.P. Mahowald. 1990. Genetic evidence that the *ovo* locus is involved in *Drosophila* germ line sex determination. *Genetics* **125:** 535–550.

Oliver, B., J. Singer, V. Laget, G. Pennetta, and D. Pauli. 1994. Function of *Drosophila ovo+* in germline sex determination depends on X-chromosome number. *Development* **120:** 3185–3195.

Parr, B.A. and A.P. McMahon. 1995. Dorsalizing signal *Wnt-7*a required for normal polarity of D-V and A-P axes of mouse limb. *Nature* **374:** 350–353.

Pauli, D. and A.P. Mahowald. 1990. Germline sex determination in *Drosophila melanogaster. Trends Genet.* **6:** 259–264.

Pauli, D., B. Oliver, and A.P. Mahowald. 1993. The role of the *ovarian tumor* locus in *Drosophila melanogaster* germline sex determination. *Development* **119:** 123–134.

Pelletier, J., W. Bruening, C.E. Kashtan, S.M. Mauer, J.C. Manivel, J.E. Striegel, D.C. Houghton, C. Junien, R. Habib, L. Fouser, R.N. Fine, B.L. Silverman, D.A. Haber, and D. Housman. 1991. Germline mutations in the Wilms' tumor suppressor gene are associated with abnormal urogenital development in Denys-Drash syndrome. *Cell* **67:** 437–447.

Satokata, I., G. Benson, and R. Maas. 1995. Sexually dimorphic sterility phenotypes in Hoxa10-deficient mice. *Nature* **374:** 460–463.

Saxen, L. 1987. Organogenesis of the kidney. *Dev. Cell Biol. Ser.* **19**.

Schaeren-Wiemers, N. and A. Gerfin-Moser. 1993. A single protocol to detect transcript of various types and expression levels in neural tissue and cultured cells: In situ hybridization using digoxigenin-labelled cRNA probes. *Histochemistry* **100:** 431–440.

Sinke, R.J., D.O. Weghuis, R.F. Suijkerbuijk, A. Tanigami, Y. Nakamura, C. Larsson, G. Weber, B. de Jong, J.W. Oosterhuis, W.M. Molenarr et al. 1994. Molecular characterization of a recurring complex chromosomal translocation in two human extragonadal germ cell tumors. *Cancer Genet. Cytogenet.* **73:** 11–16.

Sundberg, J.P. and K.S. Brown. 1994. Imperforate vagina and mucometra in inbred laboratory mice. *Lab. Anim. Sci.* **44:** 380–382.

Torres, M., E. Gomez-Pardo, G.R. Dressler, and P. Gruss. 1995. *Pax-2* controls multiple steps of urogenital development. *Development* **121:** 4057–4065.

Van den Berg, E., T. Dijkhuizen, S. Storkel, G. Brutel de la Riviere, A. Dam, H.J.A. Mensink, J.W. Oosterhuis, and B. de Jong. 1995. Chromosomal changes in renal oncocytomas. *Canc. Genet. Cytogenet.* **79:** 164–168.

Wei, G. and A.P. Mahowald. 1994. The germline: Familiar and newly uncovered properties. *Annu. Rev. Genet.* **28:** 309–324.

Wieschaus, E., C. Nüsslein-Wolhard, and G. Jurgens. 1984. Mutations affecting the pattern of the larval cuticle in *Drosophila melanogaster.* III. Zygotic loci on the X-chromosome and the fourth chromosome. *Wilhelm Roux's Arch. Dev. Biol.* **193:** 296–307.

Wigler, M., A. Pellicer, S. Silverstein, and R. Axel. 1978. Biochemical transfer of single-copy eucaryotic genes using total cellular DNA as donor. *Cell* **14:** 725–731.

Willert, K. and R. Nusse. 1998. Beta-catenin: A key mediator of Wnt signaling. *Curr. Opin. Genet. Dev.* **8:** 95–102.